DEVELOPMENT OF A HYBRID STABILIZATION SYSTEM FOR A FIXED-WING AIRCRAFT

N. A. Pervushina* and A. E. Poryvkin**

*,**Russian Federal Nuclear Center—Zababakhin All-Russian Research Institute of Technical Physics (VNIITF), Snezhinsk, Russia

**Snezhinsk Institute of Physics and Technology, branch of National Research Nuclear University Moscow Engineering Physics Institute (MEPhI), Snezhinsk, Russia

*,** ✉ kb2@vniitf.ru

Abstract. This paper presents a mathematical model of a hybrid controller developed for a fixed-wing aircraft stabilization system in the pitch channel. The stabilization system model is in the block diagram form. The hybrid controller is based on an additional force on the elevator and a fuzzy controller designed to adjust the magnitude of this force. A proportional relationship between the reference input of the stabilization system and the additional force is proposed. A mathematical model of the fuzzy controller tuned using a genetic algorithm is developed. The operation of the hybrid stabilization system with the tuned parameters of the fuzzy controller is simulated. According to the simulation results, the stabilization system with the new controller structure demonstrates high performance regardless of the magnitude of the specified reference input. The stabilization system structure increases the response speed in the control loop several times compared to the classical approach.

Keywords: fixed-wing aircraft, pitch channel, stabilization system, fuzzy controller, hybrid controller, genetic algorithm, mathematical modeling.

INTRODUCTION

A fixed-wing aircraft is a dynamic object flying along a trajectory in accordance with the differential equations of controlled motion, given initial conditions, atmospheric parameters, and other factors.

Any dynamic object requires high-performance control, and various control system configurations are developed accordingly. Stabilization systems (SSs)—a type of control systems—maintain a required angular position of a fixed-wing aircraft flying along a given trajectory. Conventional control methods [1–6], based on the principle of proportional-integral-derivative (PID) control, do not provide high response speed without compromising performance, and reducing the settling time in such control systems increases the overshoot. Improving response speed is necessary to ensure the operation of the control system under control mode switching, e.g., due to the application of a required load factor value on the aircraft's flight trajectory.

Various methods are used to improve the performance of control systems. In particular, the system's response speed is increased via an additional control loop, an additional force on the elevator, a fuzzy controller (FC), a hybrid controller (HC), etc.

Fuzzy algorithms, neural networks, genetic algorithms (GAs), and their combinations are classified as adaptive methods of mathematical modeling. Their important features include, e.g., the absence of prior knowledge about the system's operation and a fast response to changes in external operating conditions [7]. Developing a fuzzy controller is often a complex and labor-intensive process; however, there are many practical examples of improving the performance of control systems, such as increasing response speed [8–11]. Controller parameters are often tuned not manually but using GAs [11–13]. A successful algorithmic implementation of a nonlinear fuzzy PID controller was presented in [14]. A fuzzy controller developed for a remotely piloted aircraft was described in [15]. Based on the simulation results, the fuzzy controller demonstrated successful application, like fuzzy logic models in several studies by other authors; for example, see [16, 17]. Really, fuzzy controllers increase the control system's response speed; however, they require additional tuning under control mode switching and depending on the operating mode [11].

Another method for improving the performance of SSs is a functional analog of the pulse correction scheme [18]; it is suitable for implementation in digital onboard systems. This approach was successfully applied to improve the performance of the aircraft's SS in the pitch channel [19]. The stabilization system with such a correction loop is nonlinear.

The response speed of a control system, particularly in the pitch channel, can be increased by supplying an additional signal analogous to the pilot's force on the control stick [20–22]. Thrust control is implemented according to a similar law when the aircraft reaches a given altitude [23]. The control signal structure adopted in [24, 25] also includes a term corresponding to an additional force on the elevator to improve the performance of the SS.

Currently, modern modeling methods [26] are increasingly used for aircraft stabilization: fuzzy systems, GAs, neural networks, and various combinations thereof. For example, an FC combined with the classical control method forms the hybrid control method, or an HC [27]. Such a system adapts to changes in the plant's properties and independently modifies the control law according to logical rules (i.e., it possesses adaptiveness). Therefore, it is topical to develop mathematical models of controllers for improving the performance of control systems through the application of modern modeling methods.

In this paper, we investigate the possibility of constructing a mathematical model of a hybrid SS (SS with an HC) for an aircraft with an aerodynamic control method. The mathematical model of the HC combines the classical structure of the control signal in the pitch channel (the load factor error, the error integral, and the pitch rate signal (pitch damper)) with an additional control signal whose magnitude is generated by an FC depending on the operating mode of the SS.

The results below have been obtained via computer simulation. The aircraft flight in the Earth's atmosphere is described by a system of nonlinear ordinary differential equations with coefficients depending on the parameters of the incident airflow.

We sequentially solve the following problems:

– develop mathematical models of the plant and SS;

– develop a mathematical model of the SS with an additional force on the elevator;

– develop mathematical models of the HC and FC as part of the HC;

– develop a GA for tuning the FC parameters;

– recommend on tuning the FC parameters to optimize the process of developing and tuning the HC in the SS, and test the operation of the hybrid SS.

1. PROBLEM STATEMENT

The consideration below is limited to controllable fixed-wing aircraft built according to the normal aerodynamic block diagram. The object of this study is the aircraft's longitudinal control channel (pitch channel). The goal of this study is to develop a mathematical model of a hybrid stabilization system.

The plant is described by a nonlinear mathematical model in the reference frame associated with the aircraft [6, 9, 28]:

$$\begin{cases} \dfrac{d\omega_z}{dt} = \dfrac{m_z qSL}{I_{zz}} \cdot \dfrac{180}{\pi} \\ \dfrac{d\alpha}{dt} = \left(\dfrac{g \cos \vartheta}{V} - \dfrac{c_y qS}{mV} \right) \cdot \dfrac{180}{\pi} + \omega_z \\ \dfrac{d\vartheta}{dt} = \omega_z , \end{cases} \qquad (1)$$

where α is the angle of attack, deg (°); ϑ is the pitch angle, °; $m_z = m_z(\mathrm{M}, \alpha, \delta_{el}, \ldots)$ is the aerodynamic coefficient of the pitch moment, nonlinearly dependent on the parameters of the incident airflow, the elevator's angle of deflection, etc., a dimensionless quantity; $c_y = c_y(\mathrm{M}, \alpha, \delta_{el}, \ldots)$ is the aerodynamic coefficient of the lifting force, nonlinearly dependent on the parameters of the incident airflow, the elevator's angle of deflection, etc., a dimensionless quantity; M is the Mach number; q is the dynamic pressure, Pa; S is the wing area, m^2; L is the characteristic linear dimension of the aircraft, m; m is the aircraft mass, kg; V is the aircraft airspeed, m/s; finally, g = 9.80665 m/s^2 is the gravitational acceleration.

The relationship between the load factor and the angle of attack is given by [3]

$$n_y = \left(c_y^{\alpha} Sq / mg \right) \alpha = K_{\alpha} \alpha . \qquad (2)$$

The mathematical model of the hybrid stabilization system developed here is based on the classical structure of the SS in the pitch channel [6, 9]. The term corresponding to an additional force on the elevator is added to the classical structure [20–25]:

$$\sigma_{\text{el}} = \sigma_{\text{add}} + K_i \int_{t_0}^{t} \Delta n_y dt + K_n \Delta n_y - K_{\omega_z} \omega_z \,, \qquad (3)$$

where Δn_y is the load factor error, $\Delta n_y = n_{y\,\text{giv}} - n_y$; $n_{y\,\text{giv}}$ is a given load factor value; n_y is the SS output; σ_{el} is the equivalent elevator control signal, °; σ_{add} is the additional force on the elevator, °; K_i, K_n, and K_{ω_z} are the gains determined during the SS design stage; finally, ω_z is the pitch rate, °/s.

Figure 1 shows the block diagram of the SS in the pitch channel (load factor) with the control signal (3), where F is a low-pass filter; CA is the control actuator; δ_{el} is the equivalent elevator's angle of deflection, °; and p is the Laplace transform variable.

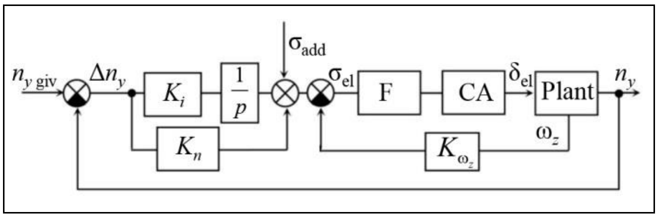

Fig. 1. The block diagram of the SS in the pitch channel with the additional force on the elevator.

The mathematical model of the control actuator and the low-pass filter is assumed to be linear:

$$T_f \frac{d\sigma_{\text{out}\,f}}{dt} + \sigma_{\text{out}\,f} = \sigma_{\text{el}}, \; T_{\text{CA}} \frac{d\delta_{\text{el}}}{dt} + \delta_{\text{el}} = \sigma_{\text{out}\,f}, \quad (4)$$

where $\sigma_{\text{out}\,f}$ is the equivalent control signal at the output of F, °; T_f is the time constant of F, s; and T_{CA} is the time constant of CA, s.

As an example, consider a flight mode with the following values: V = 100 m/s, q = 5.5 kPa, $n_{y\,\text{giv}}$ = 0.8, and $\omega_z = \pm$ 50°/s. In this mode, the transients with the classical SS structure have maximum duration.

We apply the control signal (1) to increase the response speed in the SS by adapting the value of σ_{add} via an FC to $n_{y\,\text{giv}}$, i.e., construct a hybrid SS.

Let the following requirements be imposed on the performance of the aircraft stabilization system without σ_{add}:

– For a step input disturbance of 5% of the steady-state value, the settling time t_{set} shall be approximately 1.5 s.

– The overshoot σ in the transients of the SS output signal shall be minimum, not exceeding 5%.

– The amplitude margin L_{mar} at the design stage shall be at least 10 dB.

– The phase margin φ_{mar} at the design stage shall be at least 30°.

The settling time for the hybrid SS of the aircraft shall be less than 1.5 s.

2. STABILIZATION SYSTEM DESIGN

The system of differential equations (1) can be linearized in the neighborhood of the nominal point V = 100 m/s, q = 5.5 kPa. Consider a simplified linear model of the aerodynamic coefficients c_y and m_z of the lifting force and pitch moment:

$$c_y = c_{y_0} + c_y^{\alpha}\alpha + c_y^{\delta_{\text{el}}}\delta_{\text{el}},$$
$$m_z = m_z^{\alpha}\alpha + m_z^{\delta_{\text{el}}}\delta_{\text{el}}, \qquad (5)$$

where c_{y_0} is the aerodynamic coefficient c_y for α = 0 and δ_{el} = 0, a dimensionless quantity; c_y^{α} is the derivative of the coefficient c_y with respect to the angle of attack, 1/°; $c_y^{\delta_{\text{el}}}$ is the derivative of the coefficient c_y with respect to the elevator's angle of deflection, 1/°; m_z^{α} is the derivative of the coefficient m_z with respect to the angle of attack, 1/°; finally, $m_z^{\delta_{\text{el}}}$ is the derivative of the coefficient m_z with respect to the elevator's angle of deflection, 1/°.

We linearize the system of differential equations (1) with $\Delta\vartheta \approx 0$ and the relationships (5), writing it as the continuous Laplace transform (6). For the sake of simplicity, let the dynamic parameters of the aircraft's motion be numbered following [28]: 1—the pitch rate ω_z, 2—the angle of attack α, and 3—the equivalent elevator's angle of deflection δ_{el}. Then the system of equations (1) takes the form

$$\begin{cases} a_{12}\alpha + p\omega_z = -a_{13}\delta_{\text{el}} \\ (p - a_{22})\alpha - \omega_z = -a_{23}\delta_{\text{el}}, \end{cases} \qquad (6)$$

where the coefficient $a_{12} = -m_z^{\alpha} qSL \cdot 180 / (I_z \cdot \pi)$ characterizes the static stability of the aircraft (if a_{12} > 0, then the increment in the aircraft's angular acceleration due to a deviation Δα in the angle of attack is directed opposite to this deviation, and the deviation in the angle of attack will decrease); $a_{13} = -m_z^{\delta_{\text{el}}} qSL \cdot 180 / (I_z \cdot \pi)$ characterizes the effectiveness of the elevator; $a_{22} = c_y^{\alpha} qS \cdot 180 / (mV \cdot \pi)$ characterizes the increment in the angular velocity of the tangent to the trajectory due to the deviation in the angle of attack; finally, $a_{23} = c_y^{\delta_{\text{el}}} qS \cdot 180 / (mV \cdot \pi)$ is the increment in the angular velocity of the tangent to the trajectory due to the deviation in the elevator under a constant angle of attack [29].

The transfer functions (TFs) of the plant from the input disturbance δ_{el} to the load factor n_y and pitch rate ω_z are obtained from system (6), taking the relationships (5) into account:

$$W_{\delta_{el}}^{n_y}(p) = K_\alpha \frac{c_1 p + c_0}{p^2 + a_1 p + a_0}, \quad W_{\delta_{el}}^{\omega_z}(p) = \frac{b_1 p + b_0}{p^2 + a_1 p + a_0}, \tag{7}$$

where $c_0 = -a_{13}$, $c_1 = -a_{23}$, $b_0 = a_{12}a_{23} - a_{13}a_{22}$, $b_1 = -a_{13}$, $a_1 = a_{22}$, and $a_0 = a_{12}$ are the TF coefficients.

The model values of the coefficients of the TFs (7) and the coefficients of equations (2) and (4) are provided in Table 1.

The plant's model is linear if it is described by a linear system of differential equations (6). The plant is nonlinear if its mathematical model represents a system of nonlinear differential equations (1) and the model of the aerodynamic coefficients is also nonlinear.

For the block diagram in Fig. 1, the SS can be designed by classical methods without the additional force σ_{add}, based on a reference system with given performance and stability indicators. Due to the additional input disturbance σ_{add}, it becomes impossible to obtain a single TF of the closed-loop SS. The output variable of the loop in Fig. 1 is formed as follows:

$$W_{\sigma_{add}}^{n_y}(p)\,\sigma_{add} + W_{n_{y\,giv}}^{n_y}(p)\,n_{y\,giv} = n_y,$$

where $W_{\sigma_{add}}^{n_y}(p)$ is the TF from the input disturbance σ_{add} to the load factor n_y (without considering $n_{y\,giv}$); $W_{n_{y\,giv}}^{n_y}(p)$ is the TF from the reference input $n_{y\,giv}$ to the load factor n_y (the transfer function of the closed-loop SS for the load factor, $W_{cl}(p)$).

According to the block diagram (Fig. 1) and the transfer functions (3) and (7), we obtain $W_{\sigma_{add}}^{n_y}(p)$ and $W_{n_{y\,giv}}^{n_y}(p) = W_{cl}(p)$:

$$W_{\sigma_{add}}^{n_y}(p) = \frac{D_2 p^2 + D_1 p}{p^5 + A_4 p^4 + A_3 p^3 + A_2 p^2 + A_1 p + A_0}, \tag{8}$$

$$W_{cl}(p) = \frac{B_2 p^2 + B_1 p + B_0}{p^5 + A_4 p^4 + A_3 p^3 + A_2 p^2 + A_1 p + A_0},$$

where $D_2 = K_\alpha c_1/(T_f T_{CA})$; $D_1 = K_\alpha c_0/(T_f T_{CA})$; $B_2 = K_\alpha K_n c_1/(T_f T_{CA})$; $B_1 = K_\alpha (K_i c_1 + K_n c_0)/(T_f T_{CA})$; $B_0 = (K_\alpha K_i c_0)/(T_f T_{CA})$; $A_4 = a_1 + (T_f + T_{CA})/(T_f T_{CA})$; $A_3 = a_0 + (a_1(T_f + T_{CA}) + 1)/(T_f T_{CA})$; $A_2 = ((T_f + T_{CA})a_0 + a_1 + K\omega_z b_1)/(T_f T_{CA}) + B_2$; $A_1 = (a_0 + K\omega_z b_0)/(T_f T_{CA}) + B_1$; and $A_0 = B_0$.

The SS in the pitch channel (Fig. 1) without the input disturbance σ_{add} is designed by the method of logarithmic amplitude responses [30] in accordance with the transfer function of the open-loop system:

$$W_{op}(p) = \frac{B_2 p^2 + B_1 p + B_0}{p^5 + A_4 p^4 + A_3 p^3 + (A_2 - B_2)p^2 + (A_1 - B_1)p}.$$

The resulting values of the gains K_i, K_n and K_{ω_z}, as well as the performance indicators and the amplitude L_{mar} and phase φ_{mar} margins, are presented in Table 2.

The additional force σ_{add} in the steady-state mode has no effect on the SS output n_y. By the final value theorem [31] and formula (8), for the input disturbance $1(t)$ (a unit step), we have

$$n_y(\infty) = 0 / A_0 = 0.$$

The value of σ_{add} affects only the SS transients; therefore, the SS performance can be adjusted by changing this value.

Table 1

The transfer function coefficients of the SS

Dynamic coefficient	a_1, 1/s	a_0, 1/s^2	b_1, 1/s^2	b_0, 1/s^3	c_0, 1/s^2	c_1, 1/s	K_α, 1/°	T_f, s	T_{RP}, s
Value	0.5	14	– 21	– 9.5	– 0.06	– 21	0.09	0.02	0.025

Table 2

The SS designed without the additional force σ_{add}

Parameter	K_i, °/s	K_n, °	K_{ω_z}, s	t_{set}, s	σ, %	L_{mar}, dB	φ_{mar}, °
Value	– 15.5	– 4.7	– 0.3	1.8	0	20	76

The response of the SS with the linear plant was simulated by varying the input disturbance σ_{add} between –5° and +5° under $n_{y\ giv} = 0$. The simulation results are shown in Fig. 2a: the upper curve corresponds to $\sigma_{add} = -5°$ whereas the lower one to $\sigma_{add} = 5°$. Figure 2b demonstrates the SS transients depending on the value of σ_{add}. The dashed line indicates the transient under $\sigma_{add} = 0$. And the bold line indicates the best result in terms of transient performance after introducing σ_{add}: $\sigma = 0\%$, and the response speed is higher than under $\sigma_{add} = 0$.

According to the simulation results, the optimal additional force on the elevator is about $\sigma_{add} = -3°$.

Figure 2c presents the final simulation result separately: the dashed line corresponds to the initial SS with $\sigma_{add} = 0$; the bold line, to the SS with $\sigma_{add} = -3°$; the gray line, to the SS with $\sigma_{add} = -3°$ under $n_{y\ giv} = 0$. The transient performance obtained by introducing the additional force σ_{add} ($t_{set} = 0.8$ s and $\sigma = 0\%$) is unachievable using the classical method. Reducing the settling time always increases the overshoot and, consequently, makes the system more likely to oscillate.

To confirm this conclusion, the SS was designed using the classical algorithm with the desired settling time $t_{set\ d} = 0.8$ s. The resulting overshoot was $\sigma > 20\%$. For the sake of comparison, Fig. 3 shows the following simulation results: the initial SS with $\sigma_{add} = 0$ (the dashed line), the SS with $\sigma_{add} = -3°$ (the bold line), and the SS designed with $t_{set\ d} = 0.8$ s (the gray line).

Finally, the simulation results in Fig. 4 correspond to the SS in the pitch channel with the nonlinear plant under the condition $n_{y\ giv} \le 0.7$. The transient performance with $\sigma_{add} = -3°$ deteriorates when decreasing the reference input $n_{y\ giv}$ (the desired load factor value),

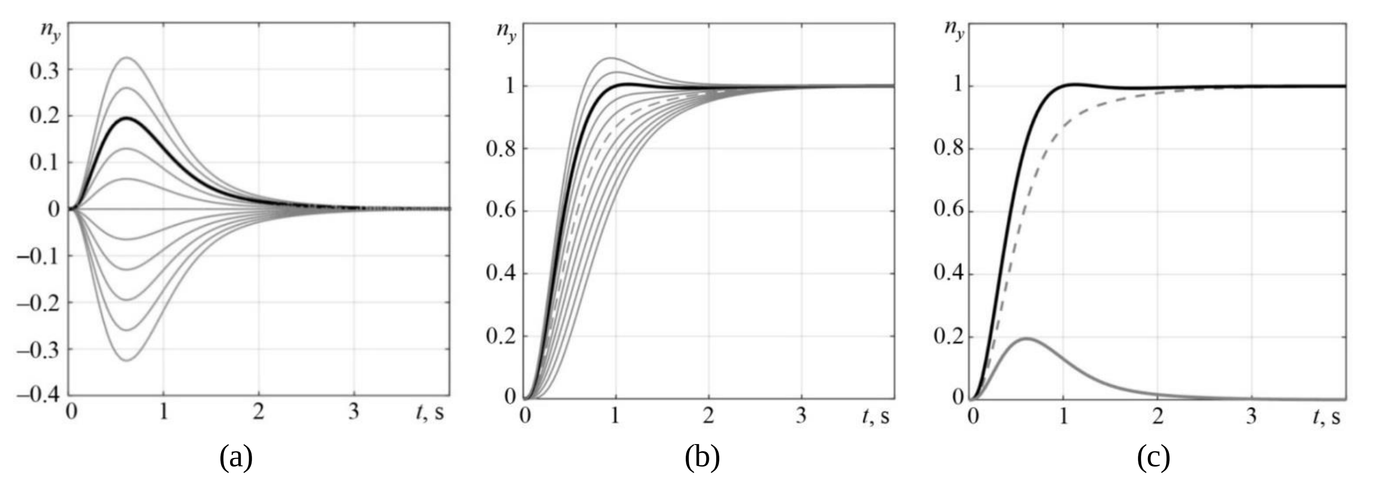

Fig. 2. The SS response to input disturbances: (a) the response to the additional force σ_{add}, (b) transients with the additional force on the elevator, and (c) transients with the optimal force value $\sigma_{add} = -3°$.

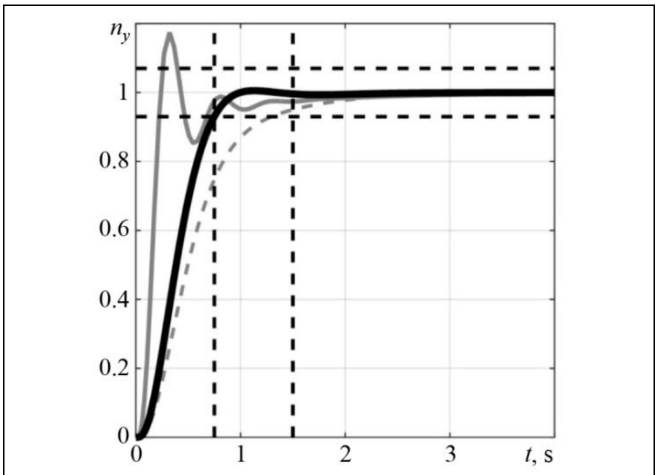

Fig. 3. Simulation results for the SS designed with desired settling times of 0.8 s and 1.5 s (see the SS performance requirements in Section 1).

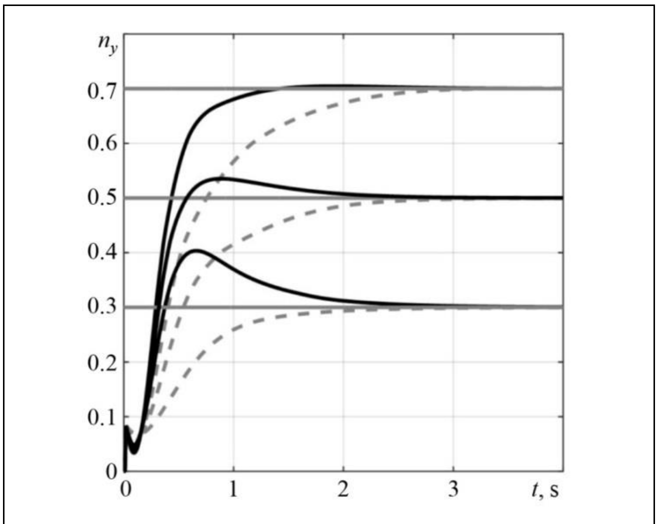

Fig. 4. Simulation results with the nonlinear plant.

see the bold line. In particular, the overshoot grows significantly, indicating an excessive effect of σ_{add}. Therefore, it is assumed that the additional force σ_{add} shall depend on $n_{y\,giv}$, e.g., linearly:

$$\sigma_{add} = K\, n_{y\,giv}, \tag{9}$$

where K is a proportionality coefficient, °.

3. FUZZY CONTROLLER DESIGN FOR TUNING THE ADDITIONAL FORCE ON THE ELEVATOR

During computer simulations, it was established that $K < 0$ regardless of the sign of $n_{y\,giv}$. For example, the gain K (9) can be tuned depending on the value $n_{y\,giv}$ as follows: if $n_{y\,giv}$ is "large" ("small"), then K shall be increased (decreased, respectively).

Forming the value of K may require considering the pitch rate ω_z. The fuzzy logic for tuning the gain K depending on the value of ω_z can, e.g., be described linguistically by the following rules:

"If ω_z is 'large,' then the value of K is decreased."

"If ω_z is 'small,' then the value of K is increased."

Based on the above considerations, we design an FC with two inputs, $n_{y\,giv}$ and ω_z, to tune the gain K (Fig. 5). The classical control signal structure remains the same, but the parameter σ_{add} is tuned using the FC. A combination of fuzzy and classical controllers constitutes a hybrid controller [27].

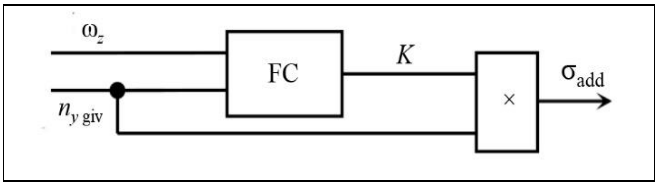

Fig. 5. A fuzzy controller for tuning σ_{add}.

The term graphs (membership function plots) of the FC variables are shown in Fig. 6.

In Fig. 6, the symbols x_i indicate the boundaries of the terms of the corresponding parameters. The terms are designated as follows: NL—"negative large," N—"negative," NS—"negative small," Z—"zero," P—"positive," and PL—"positive large."

The rule base of the FC for tuning the gain K is presented in Table 3. The superscripts here denote the rule numbers in the base.

We assign the term boundaries for the input and output parameters. Let us introduce the following arrays of the boundaries: for the input variable $n_{y\,giv}$, $A = [A_1\ A_2\ A_3\ A_4\ A_5\ A_6\ A_7]$; for the input variable ω_z, $B = [B_1\ B_2\ B_3\ B_4\ B_5\ B_6\ B_7]$; for the output variable K, $K = [K_1\ K_2\ K_3\ K_4\ K_5]$.

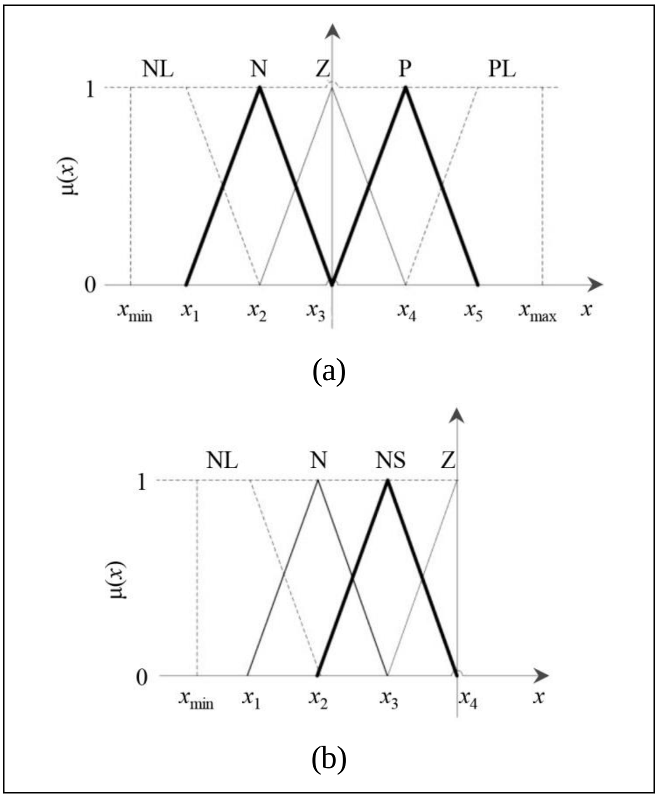

Fig. 6. Term sets for (a) the input variables $n_{y\,giv}$ and ω_z and (b) the output variable K.

Table 3

The rule base of the FC

$n_{y\,giv}$	ω_z				
	NL	N	Z	P	PL
NL	Z^1	N^2	NL^3	Z^4	Z^5
N	NS^6	N^7	NL^8	Z^9	Z^{10}
Z	N^{11}	NL^{12}	NL^{13}	NL^{14}	N^{15}
P	Z^{16}	Z^{17}	NL^{18}	N^{19}	NS^{20}
PL	Z^{21}	Z^{22}	NL^{23}	N^{24}	Z^{25}

The FC with the rule base (Table 3) was developed as a functional block in a standard environment for programming and engineering computation. Fuzzy inference was implemented using the Mamdani mechanism with center-of-gravity defuzzification [10, 32].

The term boundaries for the input variables $n_{y\,giv}$ and ω_z and the output variable K shall be specified in accordance with the operating conditions of the SS: $n_{y\,giv} < 0.8$ and $|\omega_z| < 50°/s$. For the output variable of the FC, the term boundaries shall also depend on the operating mode; due to formula (9), the left boundary shall satisfy

$$K_{min} \geq \sigma_{add}/n_{y\,giv}. \tag{10}$$

Based on the autonomous testing results of the FC functional block, the term boundaries were selected manually; see Tables 4 and 5.

Table 4

Term boundaries for the input parameters of the FC

Term boundaries	Parameter $n_{y\,\text{giv}}$							Parameter ω_z, °/s						
	A_1	A_2	A_3	A_4	A_5	A_6	A_7	B_1	B_2	B_3	B_4	B_5	B_6	B_7
Value	–0.8	–0.66	–0.33	0	0.33	0.66	0.8	–50	–30	–15	0	15	30	50

Table 5

Term boundaries for the output parameter of the FC

Term boundaries	Parameter K, °				
	K_1	K_2	K_3	K_4	K_5
Value	–7.0	–2.0	–1.5	–1	0

The designed FC was autonomously tested under different values of the input variables $n_{y\,\text{giv}}$ and ω_z. For a particular combination of these FC parameters, the value of the output parameter K was recorded. As an example, Table 6 provides the results of computer simulations of the FC for $n_{y\,\text{giv}} = \pm\ 0.7$ and $\omega_z = –50…+50$°/s. Table 6 presents the corresponding value of the output variable K of the FC, together with the value of σ_{add} calculated by formula (9).

Table 6

Autonomous testing results for the FC: an example

$n_{y\,\text{giv}}$	ω_z, °/s	K, °	σ_{add}, °
±0.7	0	∓ 4.390	–3.073
	±10	∓ 3.860	–2.702
	±20	∓ 1.104	–0.773
	±30, ±40, ±50	∓ 0.357	–0.250

Some examples illustrating the operation of the fuzzy inference system of this controller (the graphs of the output variable, with the defuzzification result indicated) can be found in Fig. 7.

For $\omega_z = 0$ and $n_{y\,\text{giv}} < 0.8$, the additional force σ_{add} on the elevator shall be approximately –3°; therefore, due to formula (10), the value of K shall exceed –3.75. Based on the results in Table 6 and Fig. 7, we conclude that the FC is effective and the gain K is calculated correctly.

The reduction of K with increasing ω_z indicates the appropriate logical principles incorporated into the rule base. Thus, the autonomous testing of the FC confirmed its effectiveness.

4. SIMULATION RESULTS FOR THE HYBRID STABILIZATION SYSTEM

Figure 8 shows the block diagram of the hybrid stabilization system with the FC for tuning the additional force σ_{add}.

The effectiveness of the hybrid SS was verified through computer simulations using both linear and nonlinear plants. The system of equations (6) or (2) was integrated using the fourth-order Runge–Kutta method, with an integration step of 0.01 s, following a convention for the numerical simulations of aircraft flight dynamics.

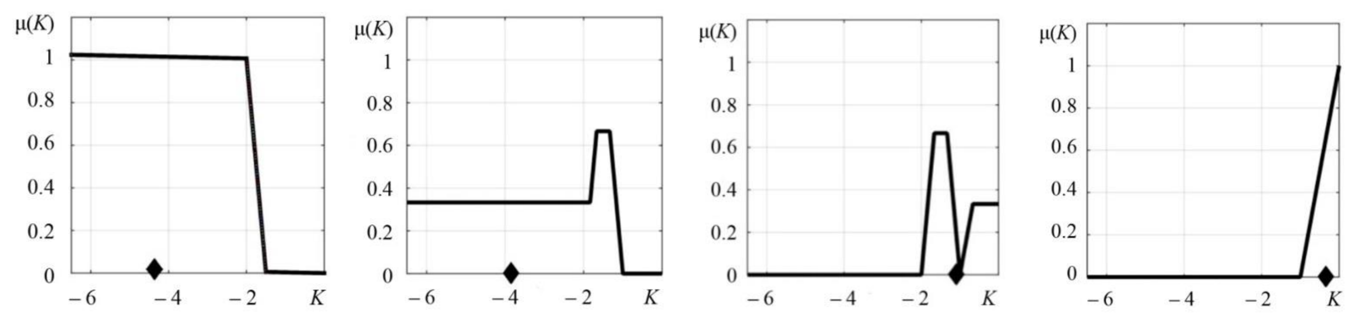

(a) (b) (c) (d)

Fig. 7. The operation of the fuzzy inference system of the FC: (a) the input $\omega_z = 0$, $n_{y\,\text{giv}} = 0.7$, and the output $K = –4.39$; (b) the input $\omega_z = 10$, $n_{y\,\text{giv}} = 0.7$, and the output $K = –3.86$; (c) the input $\omega_z = 20$, $n_{y\,\text{giv}} = 0.7$, and the output $K = –1.10$; and (d) the input $\omega_z = 30$, $n_{y\text{back}} = 0.7$, and the output $K = –\ 0.36$.

4.1. Simulation Results with the Manually Tuned FC

Figure 9 shows the simulation results for the hybrid SS with the manually tuned FC (see Section 3). Here, the solid line corresponds to the result with the FC; the dashed line, to the result without σ_{add}; the gray line, to the result with $\sigma_{add} = -3°$.

Tables 7 and 8 present performance indicators for the results shown in Fig. 9. The integral square error (ISE) was taken as an integral measure [30]:

$$ISE = \int_{t_0}^{t} \Delta n_y^2 dt \qquad (11)$$

According to the simulation results, the SS with the HC has a nearly 2 times faster response than that with the classical control method. The ISE value decreased by an average of 30% for the SS with the nonlinear plant. The system remains well-damped: the overshoot is close to zero.

Note that the FC within the HC was tuned manually, i.e., the term boundaries for the input and output variables were selected experimentally. Selecting and tuning FC parameters is a complex and labor-intensive process.

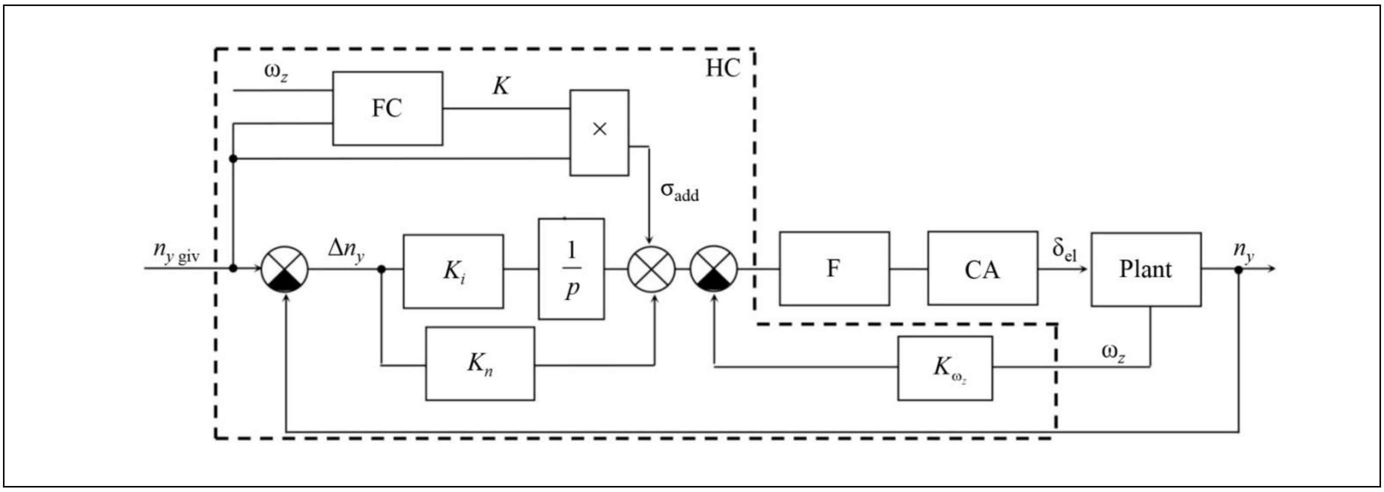

Fig. 8. The block diagram of the SS in the pitch channel with the hybrid controller.

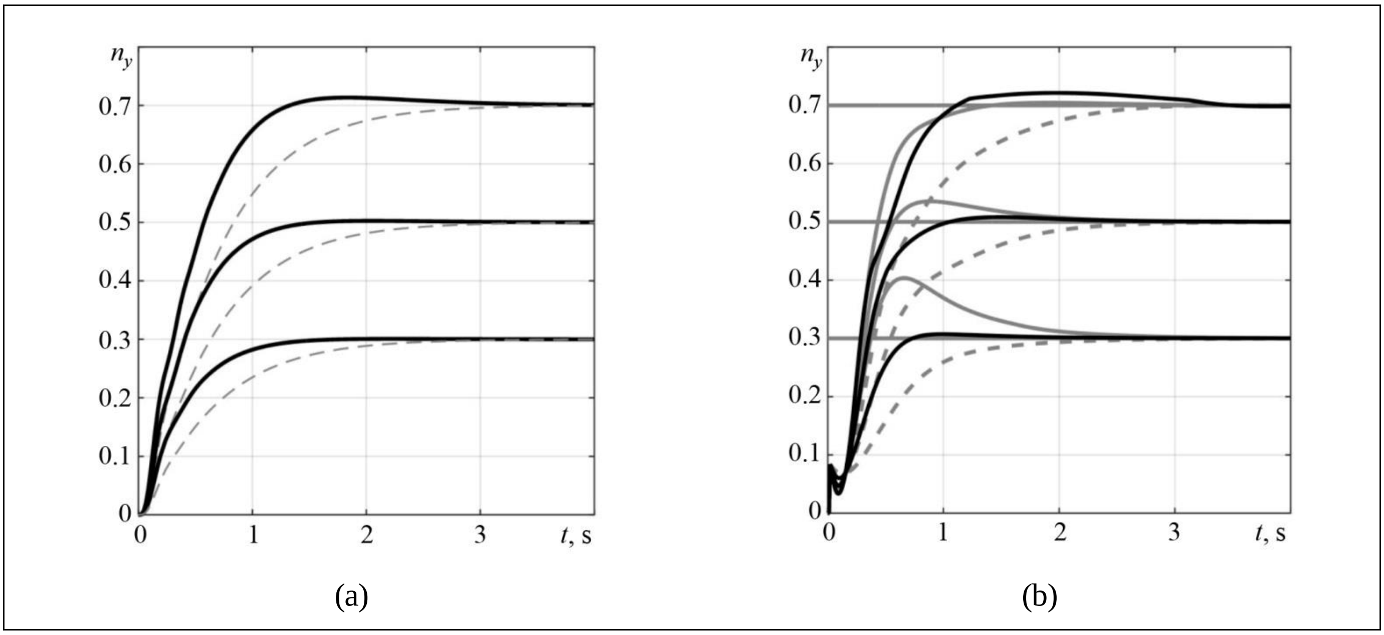

Fig. 9. The operation of the hybrid SS with the manually tuned FC: (a) the linear plant and (b) the nonlinear plant.

Table 7

Transient performance indicators for the SS with the linear plant

$n_{y\ \text{giv}}$	SS without the additional force on the elevator ($\sigma_{\text{add}} = 0$)			SS with the hybrid controller ($\sigma_{\text{add}} \neq 0$)		
	t_{set}, s	σ, %	*ISE*, s	t_{set}, s	σ, %	*ISE*, s
0.7	1.8	0	0.1183	1.0	1.9	0.1002
0.5	1.8	0	0.0548	1.0	0	0.0455
0.3	1.8	0	0.0177	1.0	0	0.0144

Table 8

Transient performance indicators for the SS with the nonlinear plant

$n_{y\ \text{giv}}$	SS without the additional force on the elevator ($\sigma_{\text{add}} = 0$)			SS with the hybrid controller ($\sigma_{\text{add}} \neq 0$)		
	t_{set}, s	σ, %	*ISE*, s	t_{set}, s	σ, %	*ISE*, s
0.7	1.7	0	0.1774	0.90	3.0	0.1301
0.5	1.7	0	0.0836	0.85	1.6	0.0562
0.3	1.5	0	0.0264	0.61	0.5	0.0169

4.2. The Structure and Operating Principle of the Genetic Algorithm Proposed

The idea is to tune the FC using a GA. A genetic algorithm of a similar structure was developed and successfully applied to tune an FC earlier [13]. The GA presented below tunes the FC parameters in the SS with the nonlinear plant. The genetic algorithm works only in the deterministic mode when a starting chromosome (initial parameter settings) is available; gene mutations are random and vary for each genotype (a set of genes characterizing the FC parameter). The "best" chromosome is selected by minimizing the ISE and the overshoot σ.

The operations of the genetic algorithm.

1. A starting chromosome H is formed by three groups of genes (genotypes): G_1, the (1×7)-dimensional array containing the term boundaries $[n_{y\ \text{giv}}^1, n_{y\ \text{giv}}^2]$ for $n_{y\ \text{giv}}$; G_2, the (1×7)-dimensional array containing the term boundaries $[\omega_z^1, \omega_z^2]$ for ω_z; and G_3, the (1×5)-dimensional array containing the term boundaries $[K^1, K^2]$ for term K:

$$H = \{G_1, G_2, G_3\}.$$

The arrays of the term boundaries are given in Tables 4 and 5.

2. The value ISE_0 of the fitness function (11) is computed.

3. The number k of GA steps to obtain the optimal solution is set.

4. The second chromosome $H' = \{G_1', G_2', G_3'\}$ of the initial population is formed by mutating the genes from G_1, G_2, and G_3. The number of genes n_1, n_2, and n_3 for mutation can be varied.

5. Crossover (mixing of gene groups) is applied to two chromosomes from the populations H and H', producing the following combinations: $\{G_1, G_2, G_3\}$, $\{G_1', G_2, G_3\}$, $\{G_1, G_2', G_3\}$,…, $\{G_1', G_2', G_3'\}$. As a result, eight chromosomes of the new generation are obtained.

6. The fitness of the chromosomes in the current population is estimated using the function (11), and the best chromosome with *ISE* less than ISE_0 is selected. When selecting the best chromosome, the overshoot σ is also estimated. If σ = 0, then the best chromosome becomes the starting one, and $ISE_0 = ISE$.

7. The termination condition is checked: the number of best chromosomes selected must be k. If this condition fails, the initial population continues to be formed by returning to Operation 4.

The GA finds the optimal solution by sequentially selecting the best chromosomes in k steps.

As established during the simulations, ten steps ($k = 10$) are sufficient to obtain the optimal solution. For a greater number of steps, the number of iterations grows significantly, but the final result slightly differs from that at the previous step in terms of the ISE value and the performance of the SS.

As an example, the FC parameters tuned by the GA with $n_{y\ \text{giv}} = 0.7$ and $k = 10$ are presented in Fig. 10a and Table 9. In Fig. 10a, the bold line corresponds to the best result; the dashed line, to the result with the manually tuned FC; the thin black line, to the result without the additional force σ_{add}; the gray color, to the intermediate variants before obtaining the optimal solution for $k = 10$.

The transient performance indicators of the hybrid SS with the nonlinear plant, with the manually tuned FC and the one tuned by the genetic algorithm, are given in Table 10. The transient graphs are provided in Fig. 10b.

Note that the hybrid SS was tuned for the maximum input disturbance $n_{y\,\mathrm{giv}} = 0.7$, but the tuning procedure ensured the same performance of the SS for $n_{y\,\mathrm{giv}} < 0.7$ as well ($t_{\mathrm{set}} \approx 0.6$ s and $\sigma < 1\%$).

4.3. Simulation Results for the Hybrid SS after Tuning

The effectiveness of the hybrid SS in the aircraft flight mode under consideration (V = 100 m/s and q = 5.5 kPa) after tuning the FC parameters by the GA was demonstrated under stabilization mode switching. For comparison, the graphs in Fig. 11 show the performance of the classical and hybrid SS (the thin and bold lines, respectively).

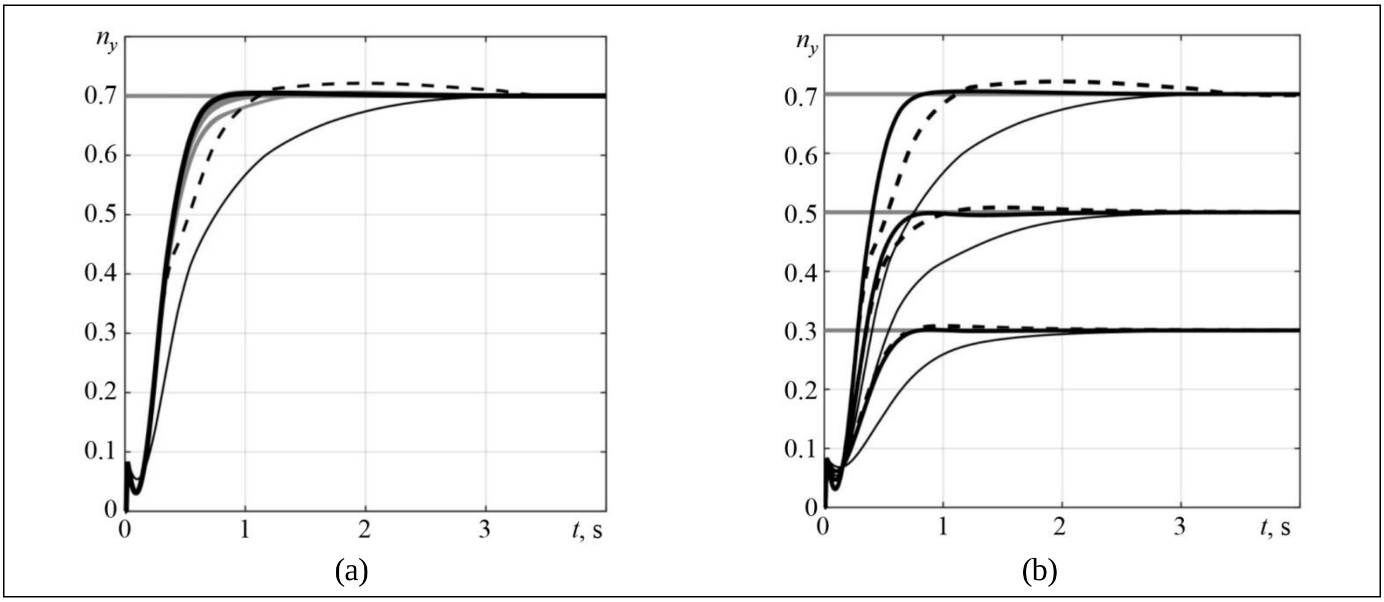

Fig. 10. The operation of the hybrid SS with the nonlinear plant: (a) the FC parameters optimized by the GA and (b) under different values of $n_{y\,\mathrm{giv}}$.

Table 9

GA results for tuning the FC parameters: $n_{y\mathrm{giv}}$ = 0.7 and k = 10

No.	The number of GA iterations	Best chromosome H			*ISE* in 4 s
		Genotype G_1 (term boundaries for $n_{y\,\mathrm{giv}}$)	Genotype G_2 (term boundaries for ω_z)	Genotype G_3 (term boundaries for K)	
1	1	[–0.800 –0.548 0 0.732 0.744 0.753 0.800]	[– 50.00 – 30.00 – 15.00 15.00 15.57 29.22 50.00]	[– 7.000 – 2.000 – 1.500 – 1.000 0]	0.12063
2	11	[– 0.800 – 0.548 0 0.732 0.744 0.753 0.800]	[–50.00 –6.761 –4.620 15.00 15.57 32.53 50.00]	[– 7.000 – 2.000 – 1.500 – 1.000 0]	0.12056
3	14	[– 0.800 – 0.548 0 0.732 0.744 0.753 0.800]	[–50.00 –6.761 –4.620 15.00 15.57 32.53 50.00]	[– 7.000 – 3.087 – 1.021 – 1.000 0]	0.12022
4	9	[– 0.800 – 0.548 0 0.732 0.744 0.753 0.800]	[–50.00 –4.620 –4.211 15.00 15.57 43.57 50.00]	[– 7.000 – 3.087 – 1.021 – 1.000 0]	0.12016
5	4	[– 0.800 – 0.548 0 0.732 0.744 0.753 0.800]	[– 50.00 – 47.00 15.00 30.45 43.57 48.61 50.00]	[– 7.000 – 6.531 – 1.021 – 1.000 0]	0.11771
6	2	[– 0.800 – 0.548 0 0.732 0.744 0.753 0.800]	[–50.00 –47.00 15.00 30.45 43.57 48.61 50.00]	[– 7.000 – 6.701 – 1.603 – 1.021 0]	0.11710
7	2	[– 0.800 – 0.548 0 0.732 0.744 0.753 0.800]	[–50.00 –47.00 15.00 30.45 43.57 48.61 50.00]	[– 7.000 – 6.701 – 1.751 – 1.154 0]	0.11688
8	8	[– 0.800 – 0.548 0 0.732 [0.744. 0.753. 0.800]	[–50.00 –47.00 15.00 30.45 43.57 48.61 50.00]	[–6.701 –5.974 –2.582 –1.751 0]	0.11686
9	1	[– 0.800 – 0.548 0 0.732 0.744 0.753 0.800]	[–50.00 –47.00 15.00 30.45 43.57 48.61 50.00]	[– 6.701 – 5.974 – 3.277 – 1.751 0]	0.11635
10	1	[– 0.800 – 0.548 0 0.732 0.744 0.753 0.800]	[– 50.00 – 47.00 15.00 30.45 [43.57 48.61 50.00]	[– 6.701 – 6.235 – 3.277 – 2.061 0]	0.11609

Table 10

Transient performance indicators for the SS with the nonlinear plant

$n_{y\ \mathrm{giv}}$	SS with the hybrid controller (FC tuned manually)			SS with the hybrid controller (FC tuned by the GA)		
	t_{set}, s	σ, %	*ISE*, s	t_{set}, s	σ, %	*ISE*, s
0.7	0.90	3.0	0.1301	0.61	0.7	0.1161
0.5	0.85	1.6	0.0562	0.62	0	0.0553
0.3	0.61	0.5	0.0169	0.63	0.4	0.0169

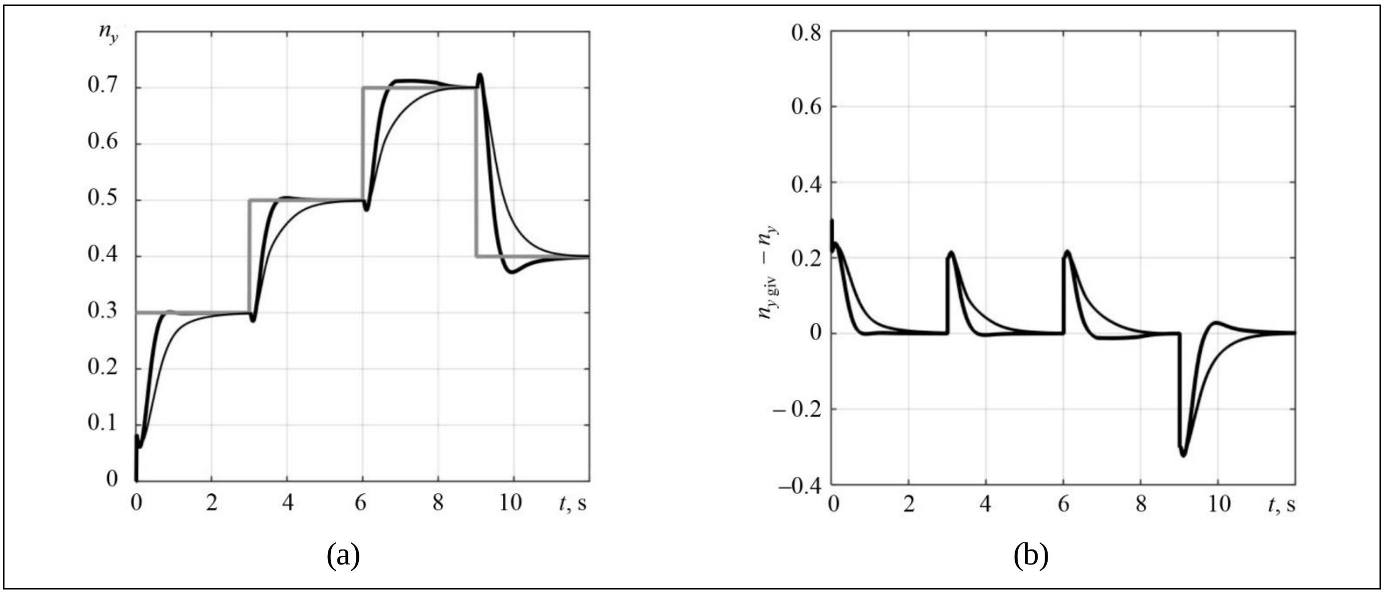

Fig. 11. The operation of the classical and hybrid SSs with the nonlinear plant: (a) processes at the SS output and (b) the deviations of the factual values of n_y from $n_{y\ \mathrm{giv}}$.

According to the graphs in Fig. 11, the hybrid SS rapidly reduces the error. It is reasonable to apply the HC to improve the SS performance, as illustrated by the model problem in the pitch channel.

CONCLUSIONS

A mathematical model of a hybrid stabilization system (SS) for a fixed-wing aircraft with aerodynamic control in the pitch channel has been developed. It is based on an additional force on the elevator introduced into the control loop and a hybrid controller (HC) combining a fuzzy controller (FC) and the classical control scheme.

The nonlinear plant has been simulated under various step input disturbances; according to the simulation results, the SS demonstrates worse performance for a fixed magnitude of the additional force. In this regard, it has been proposed to establish a proportional relationship between the input disturbance and the magnitude of the additional force. In particular:

– A proportionality coefficient has been introduced.

– Linguistic rules have been constructed to tune the coefficient depending on the specified input disturbance and the pitch rate.

– An FC has been designed.

– The FC parameters have been tuned manually.

The autonomous testing of the FC, as well as its testing as part of the hybrid SS, has confirmed the effectiveness of this controller. A genetic algorithm (GA) has been developed to optimize the tuning process of the FC parameters. As has been found, ten steps of the GA are sufficient to obtain the optimal solution (the optimal FC parameters).

Based on the computer simulation results, the SS with the HC has a high response, i.e., a settling time of approximately 0.6 s without overshoot.

The mathematical model of the fuzzy controller and the genetic algorithm have been implemented as program code. According to the simulation results, the proposed hybrid SS structure adapts to the specified reference input. The loop with the classical control signal structure is designed in a standard manner, while the FC parameters are tuned by the GA in a short time.

The design approach to hybrid SSs proposed in this paper is recommended for the development of adaptive stabilization systems for fixed-wing aircraft with aerodynamic pitch control, in cases where it is necessary to improve the SS performance under various reference inputs. An important advantage of the hybrid control method over the classical one is its response speed and the overall improvement in stabilization quality.

REFERENCES

1. Bochkarev, A.F., Andreevskii, V.V., Belokonov, V.M., et al., *Aeromekhanika samoleta: Dinamika poleta* (Airplane Aeromechanics: Flight Dynamics), Moscow: Mashinostroenie, 1985. (In Russian.)
2. Raspopov, V.Ya., *Datchiki i sistemy avioniki BLA* (Avionics Sensors and Systems of UAVs), Moscow: Mashinostroenie, 2010. (In Russian.)
3. Ostoslavskii, I.V. and Strazheva, I.V., *Dinamika poleta. Traektorii letatel'nykh apparatov* (Flight Dynamics. Aerial Vehicle Trajectories), 2nd ed., Moscow: Mashinostroenie, 1969. (In Russian.)
4. Krasnov, N.F. and Koshevoi, V.N., *Upravlenie i stabilizatsiya v aerodinamike* (Control and Stabilization in Aerodynamics), Moscow: Vysshaya Shkola, 1978. (In Russian.)
5. Baidakov, V.B. and Klumov, A.S., *Aerodinamika i dinamika poleta letatel'nykh apparatov* (Aerodynamics and Flight Dynamics of Aerial Vehicles), Moscow: Mashinostroenie, 1979. (In Russian.)
6. Mikhalev, I.A., *Sistemy avtomaticheskogo upravleniya samoletom* (Automatic Aircraft Control Systems), Moscow: Mashinostroenie, 1971. (In Russian.)
7. Lebedeva, N.V. and Solov'ev, S.V., Intelligent Systems Application While Spacecraft Flight Operational Control, *Vestnik Mosk. Aviats. Inst.*, 2018, vol. 25, no. 2, pp. 160–171. (In Russian.)
8. Piegat, A., *Fuzzy Modeling and Control*, Heidelberg–New York: Physica-Verlag, 2001.
9. Vasil'ev, V.I. and Il'yasov, B.G., *Intellektual'nye sistemy upravleniya. Teoriya i praktika* (Intelligent Control Systems: Theory and Practice), Moscow: Radiotekhnika, 2009. (In Russian.)
10. Pervushina, N.A., Donovskii, D.E., and Khakimova, A.N., Development of Synthetic Methodology of Neuro-Fuzzy Controller Adjusted by Genetic Algorithm, *Vestnik Kontserna VKO Almaz-Antei*, 2018, no. 4, pp. 82–90. (In Russian.)
11. Pervushina, N.A. and Khakimova, A.N., Development of Mathematical Models of Fuzzy Controllers Set by Genetic Algorithm to Stabilize Dynamic Object, *Control Sciences*, 2020, no. 4, pp. 3–14. (In Russian.)
12. Signe, R.K. and Motto, F.B., Fuzzy-PID Controller Based Sliding-Mode for Suppressing Low Frequency Oscillations of the Synchronous Generator, *Heliyon*, 2024, no. 10. DOI: https://doi.org/10.1016/j.heliyon.2024.e35035
13. Li, K., Bai, Y., and Zhou, H., Research on Quadrotor Control Based on Genetic Algorithm and Particle Swarm Optimization for PID Tuning and Fuzzy Control-Based Linear Active Disturbance Rejection Control, *Electronics*, 2024, no. 13. DOI: https://doi.org/10.3390/electronics13224386
14. Burakov, M.V. and Yakovets, O.B., Fuzzy Logic Control over a Power Gyroscopic System, *Journal of Instrument Engineering*, 2015, vol. 58, no. 10, pp. 804–808. (In Russian.)
15. Lysenko, L.N., Cuong, N.D., and Chuong, F.V., Modeling of Motion of Remotely Controlled Aerial Vehicle with Modified Vague Regulator in Flight Control Contour, *Polet*, 2013, no. 2, pp. 24–30. (In Russian.)
16. Ulianov, G., Ivanov, S., and Vladyko, A.G., The Model of Controlling the Unmanned Aerial Vehicle with a Fuzzy Logic Controller, *Information and Control Systems*, 2012, no. 4, pp. 70–73. (In Russian.)
17. Matveev, E.N. and Glinchikov, V.A., Fuzzy Logic Conclusion in the Control System UAV, *Journal of Siberian Federal University. Engineering & Technologies*, 2011, no. 4, pp. 79–91. (In Russian.)
18. Obnosov, B.V., Voronov, E.M. Mikrin, E.A., et al., *Stabilizatsiya, navedenie, gruppovoe upravlenie i sistemnoe modelirovanie bespilotnykh letatel'nykh apparatov. Sovremennye podkhody i metody* (Stabilization, Guidance, Group Control, and System Modeling of Unmanned Aerial Vehicles: Modern Approaches and Methods), in 2 vols., Moscow: Bauman Moscow State Technical University, 2018. (In Russian.)
19. Pervushina, N.A. and Frolova, A.D., Designing an Adaptive Stabilizing System for an Unmanned Aerial Vehicle, *Control Sciences*, 2022, no. 5, pp. 2–12. ~~(In Russian)~~
20. Sakharchuk, D.A., Sivashko, A.B., Kruglikov, S.V., et al., Directions for the Creation and Development of Unmanned Aerial Systems, *Science Intensive Technologies*, 2014, vol. 15, no. 5, pp. 22–26. (In Russian.)
21. Zhivov, Yu.G. and Poedinok, A.M., An Adaptive Control System for Aircraft Longitudinal Motion, *Uchenye Zapiski TsAGI*, 2012, vol. XLIII, no. 5, pp. 91–100. (In Russian.)
22. Grebyonkin, A.V., Development of Trajectory Autoflare Algorithm on Landing with Spooler System Usage**,** *Trudy Mosk. Inst. Elekromekh. Avtomat. Navigats. Upravlen. Letat. Appar.*, 2013, no. 6, pp. 2–17. (In Russian.)
23. Kulikov, L.I., Flight Control Algorithm Design for a Parachute-Type Unmanned Aerial Vehicle in Loitering Mode at a Given Altitude, *Military Engineering*, 2014, vol. 266, no. 9. pp. 53–63. (In Russian.)
24. Popova, I.V., Zemskov, A.V., Lestev, A.M., and Pestova, K.S., Control algorithms for Air-To-Surface Gliding Unmanned Aerial Vehicles, *Trudy XII-go Vserossiiskogo soveshchaniya po problemam upravleniya* (Proceedings of the 12th All-Russian Meeting on Control Problems), Moscow, 2014, pp. 3681–3689. (In Russian.)
25. Bystrov, D.A., Development and Research of Adaptation and Stabilization Algorithms in the System of an Aircraft, *Modern Science: Actual Problems of Theory and Practice. Ser. Natural and Technical Sciences*, 2014, no. 5/6, pp. 3–10. (In Russian.)
26. Pashchenko, F.F., Pashchenko, A.F., Gulyaev, S.V., and Visloguzov, A.D., Application of Hybrid Methods in Intelligent Control Systems, *Sensors and Systems*, 2023, no. 2, pp. 51–58. (In Russian.)
27. *Metody robastnogo, neiro-nechetkogo i adaptivnogo upravleniya* (Methods of Robust, Neural Network-Based, and Adaptive

Control), Egupov, N.D., Ed., 2nd ed., Moscow: Bauman Moscow State Technical University, 2002. (In Russian.)

28. Lebedev, A.A. and Karabanov, V.A., *Dinamika sistem upravleniya bespilotnymi letatel'nymi apparatami* (Dynamics of Control Systems of Unmanned Aerial Vehicles), Moscow: Mashinostroenie, 1965. (In Russian.)
29. Guseinov, A.B., Lyapunov, V.V., and Trusov, V.N., *Proektirovanie sistem upravleniya krylatykh raket* (Control System Design for Cruise Missiles), Moscow: Moscow Aviation Institute, 2020. (In Russian.)
30. Besekerskii, V.A. and Popov, E.P., *Teoriya sistem avtomaticheskogo regulirovaniya* (Theory of Automatic Regulation Systems), 4th ed., St. Petersburg: Professiya, 2007. (In Russian.)
31. Aramanovich, I.G., Lunts, G.L., and El'sgol'ts, L.E., *Funktsii kompleksnogo peremennogo. Operatsionnoe ischislenie. Teoriya ustoichivosti* (Functions of a Complex Variable. Operational calculus. Stability Theory), Moscow: Nauka, 1965. (In Russian.)
32. Leonenkov, A.V., *Nechetkoe modelirovanie v srede MATLAB i fuzzyTECH* (Fuzzy Modeling in MATLAB и fuzzyTECH), St. Petersburg: BKhV Peterburg, 2005. (In Russian.)

This paper was recommended for publication by F.F. Pashchenko, a member of the Editorial Board.

Received April 9, 2025,
and revised December 4, 2025.
Accepted January 15, 2025.

Author information

Pervushina, Natal'ya Aleksandrovna. Cand. Sci. (Phys.–Math.), Russian Federal Nuclear Center—Zababakhin All-Russian Research Institute of Technical Physics (VNIITF), Snezhinsk, Russia
✉ kb2@vniitf.ru

Poryvkin, Aleksandr Evgen'evich. Research Engineer, Russian Federal Nuclear Center—Zababakhin All-Russian Research Institute of Technical Physics (VNIITF), Snezhinsk, Russia; Snezhinsk Institute of Physics and Technology, branch of National Research Nuclear University Moscow Engineering Physics Institute (MEPhI), Snezhinsk, Russia
✉ kb2@vniitf.ru

Cite this paper

Pervushina, N.A. and Poryvkin, A.E., Development of a Hybrid Stabilization System for a Fixed-Wing Aircraft. *Control Sciences* **2,** 30–42 (2026).

Translated into English by *Alexander Yu. Mazurov*,
Cand. Sci. (Phys.–Math.),
Trapeznikov Institute of Control Sciences,
Russian Academy of Sciences, Moscow, Russia
✉ alexander.mazurov08@gmail.com